Antiferromagnetism and Its Relation to the Superconducting Phases of UPt3

Isaacs, E.D.; Zschack, P.; Broholm, C.L.; Burns, C.; Aeppli, G.; Ramirez, A.P.; Palstra, T.T.M.; Erwin, R.W.; Stücheli, N.; Bucher, E.

Published in:
Physical Review Letters

DOI:
10.1103/PhysRevLett.75.1178

Antiferromagnetism and Its Relation to the Superconducting Phases of UPt_3

E. D. Isaacs,[1] P. Zschack,[2] C. L. Broholm,[3,6] C. Burns,[4] G. Aeppli,[1,6] A. P. Ramirez,[1] T. T. M. Palstra,[1] R. W. Erwin,[5] N. Stücheli,[1,*] and E. Bucher[1,†]

[1] *AT&T Bell Laboratories, Murray Hill, New Jersey 07974*
[2] *ORISE, Brookhaven Laboratory, Upton, New York 11973*
[3] *The Johns Hopkins University, Baltimore, Maryland 21218*
[4] *Western Michigan University, Kalamazoo, Michigan 49008*
[5] *National Institute of Science and Technology, Gaithersburg, Maryland 20899*
[6] *Risø National Laboratory, Roskilde, DK-4000, Denmark*

(Received 16 January 1995)

Using magnetic x-ray and neutron diffraction in UPt_3, we find that a suppression of the antiferromagnetic scattering intensity in the superconducting phase is due to a reduction in the magnitude of the staggered moment with no change in symmetry. The existence of the suppression as well as the magnetic correlation lengths are not affected by the presence or absence of a visible splitting in the superconducting transition. The simplest models wherein antiferromagnetic order provides the symmetry-breaking field for the splitting do not provide a compete explanation of our results.

PACS numbers: 74.70.Tx, 74.25.–q, 75.25.+z

UPt_3 has been clearly established as an unconventional superconductor [1]. Many measurements [2–6] demonstrate that the superconducting gap is anisotropic. Other manifestations of such unconventional superconductivity are the splitting of the superconducting transition in zero magnetic field [7] and the existence of three apparently distinct superconducting phases [8] in the H-T plane. It has been suggested, in analogy to the B phase in superfluid ^{3}He, that the zero-field splitting arises from the coupling of a superconducting order parameter with internal degrees of freedom (i.e., spin [9] or orbital [10] angular momentum) to another symmetry-breaking field in the system. The most popular candidate for such a symmetry-breaking field is the weak, finite-ranged antiferromagnetic order found below $T_N = 5$ K [11]. Two magnetic neutron scattering studies have shown that the antiferromagnetic and superconducting order parameters are indeed coupled. The first of these showed that a reduced (0.5,0,1) magnetic Bragg peak intensity characterizes the low T and H superconducting state of crystals with a broad, indiscernibly split, $H = 0$ transition [12]. The second demonstrated that pressure simultaneously suppresses the antiferromagnetic order and the zero-field splitting of the superconducting transition [13]. While informative, the two experiments leave many important questions unanswered, notably (i) whether superconductivity affects the magnetic Bragg peaks in crystals annealed to yield a split transition; (ii) if so, what change in the spin structure do the modified Bragg intensities entail; (iii) whether there is qualitatively different behavior in the near surface regime probed by important techniques such as ac susceptibility and muon spin relaxation [3,14]; and (iv) whether the observability of a split transition is related to the range of the antiferromagnetic correlations.

In this paper we address questions (i)–(iv) utilizing the polarization selection rules unique to resonant magnetic x-ray and magnetic neutron scattering and the fact that resonant x-ray scattering probes the near surface and neutrons are sensitive to the bulk. Specifically, our data reveal that superconductivity changes the amplitude but not the direction of the ordered moments in an annealed crystal of UPt_3. In addition, the data show that the effect of superconductivity on magnetism is similar in the bulk and near-surface region of etched UPt_3. Finally, the magnetic length scale, in contrast to the electronic mean free path, is at best only weakly correlated with the observability of a split superconducting transition.

UPt_3 has the hexagonal close-packed Ni_3Sn structure [15]. In this paper Bragg reflections are indexed in a hexagonal reciprocal lattice with $a^* = b^* = 4\pi/a\sqrt{3} = 1.264$ Å^{-1} and $c^* = 2\pi/c = 1.285$ Å^{-1}. For the neutron and x-ray measurements we used a 14 g, 35 mm long $\times$ 5 mm diam cylindrical crystal and a 0.8 g, 2 mm thick $\times$ 5 mm diam disk, respectively. The x-ray sample was polished and subsequently etched in HCl. The x-ray measurements were performed at beam line X14A [16] at the National Synchrotron Light Source using resonant magnetic x-ray scattering [17] in order to observe the very small ordered moment in UPt_3 [18]. At the $M_{\rm IV}$ resonance of uranium ($E = 3.725$ keV), the x-ray penetration depth is only $\sim$2500 Å. High resolution neutron diffraction was carried out on the TAS1 cold-source triple-axis spectrometer at Risø National Laboratory in Denmark. High intensity and coarse resolution measurements of the order parameter were carried out on the thermal-neutron triple-axis spectrometer, BT2, at NIST.

We grew UPt_3 crystals by the electron beam float zone method. Unannealed material of this type was used in all but one [13] of the previous neutron diffraction experiments addressing the coupling of magnetism and superconductivity. Figure 1 shows specific heat data for such a crystal in which there is a single broad super-

0031-9007/95/75(6)/1178(4)$06.00

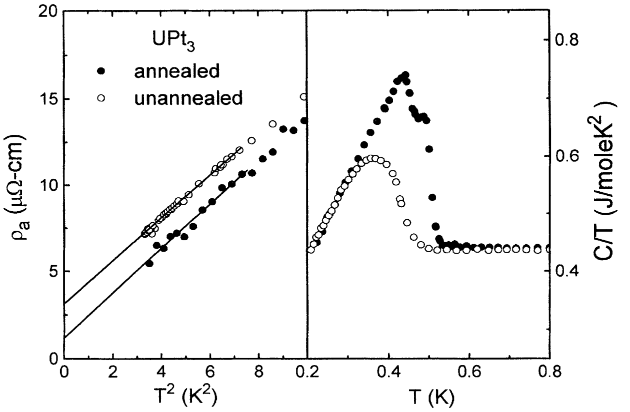

FIG. 1. Normal state resistivity (left panel) and specific heat (right panel) of unannealed (open circles) and annealed (filled circles) samples of UPt_3. Annelaing splits the superconducting transition with $T_{c-} \cong 0.46$ K and $T_{c+} \cong 0.51$ K.

conducting transition with a mean $T_c \cong 0.4$ K. After an anneal of 24 h at 1230 °C with a slow cool to 500 °C over 15 days, the same crystal displayed the specific heat represented by the filled circles in Fig. 1. The transition is now resolvably split [7,19], with $T_{c-} = 0.46$ and $T_{c+} = 0.51$ K. The annelaing also reduced the residual (extrapolated to $T = 0$) normal state resistivity ρ_0 in

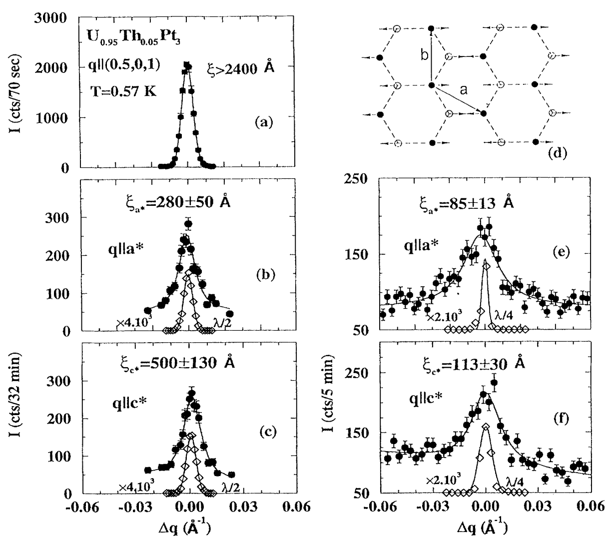

FIG. 2. (a) θ-2θ (radial), resolution limited scan through the (0.5,0,1) antiferromagnetic Bragg peak in $U_{0.95}Th_{0.05}Pt_3$. (b),(c) Neutron scattering intensity through $\mathbf{q} = (0.5, 0, 1)$ for $T = 0.57$ K (filled circles). The diamonds show diffraction of $\lambda/2$ neutrons. The solid lines are fits as described in the text. (d) Longitudinal antiferromagnetic structure of a single domain (after Ref. [21]). (e),(f) X-ray magnetic scattering scans along the $\mathbf{a}^*$ and $\mathbf{c}^*$ directions through $\mathbf{q} = (0.5, 0, 2)$ taken at $T =$ 150 mK (filled circles). The diamonds show diffraction of $\lambda/4$ photons which are shown with the calculated instrumental resolution (solid line).

the basal plane from 3.1 ± 0.5 to 1.3 ± 0.1 $\mu\Omega$ cm as shown in Fig. 1. In contrast, we find the magnetic properties to be virtually unaffected by annealing. Figures 2(b) and 2(c) show neutron scans through the (0.5,0,1) magnetic Bragg point along directions parallel and perpendicular to the basal plane. A detailed analysis, fitting Lorenztian profiles, convolved with the Gaussian experimental resolution, yields correlation lengths along $\mathbf{a}^*$ and $\mathbf{c}^*$ in the annealed sample that are $\xi_{\mathbf{a}^*} \cong 280 \pm 50$ Å and $\xi_{\mathbf{a}^*} \cong 500 \pm 130$ Å, while for the previously measured unnannealed sample, they are $\xi_{\mathbf{a}^*} \cong 295 \pm 40$ Å and $\xi_{\mathbf{c}^*} \cong 370 \pm 70$ Å. Other parameters characterizing antiferromagnetic order, namely, the Néel temperature, $T_N \cong 5$ K, and the amplitude, $\mu \cong 0.018(2)\mu_B$, of the staggered moment appear the same for annealed and unannealed crystals within experimental error. For further comparison we also show in Fig. 2(a) the nearly resolution-limited profile of the (0.5,0,1) magnetic peak in $U_{0.95}Th_{0.05}Pt_3$. The magnetic correlation length in the highly disordered alloy with a Cr-like resistance anomaly at $T_N = 6$ K [20] and the same magnetic structure as UPt_3 [21] is at least 8 times larger than for pure UPt_3.

Table I compares the absolute magnetic neutron scattering cross section of six antiferromagnetic Bragg peaks with the cross sections calculated for the simple magnetic structure shown in Fig. 2(d). The data support the previous suggestion that the antiferromagnetic structure of UPt_3 is equivalent to that observed in $U_{0.95}Th_{0.05}Pt_3$, but with an order-of-magnitude smaller moment [12]. The crucial feature of this magnetic structure is that it breaks the sixfold rotation symmetry and so separates the sample into orthorhombic magnetic domains.

Given that the magnetic order in UPt_3 has many of the earmarks of the central peak phenomenon near structural phase transitions, i.e., small amplitude, finite coherence length, and peculiar temperature dependence, it is reasonable to question its homogeneity, and in a particular to ask whether it persists near the sample surfaces. In fact, the resonant x-ray scattering data shown in Figs. 2(e) and 2(f) reveal magnetic correlation lengths that are shorter than those given by the neutron measurement shown in Figs. 2(b) and 2(c). Furthermore, Fig. 3(a) shows that the

TABLE I. Comparison of the magnetic neutron diffraction cross section, σ_n^{obs}, for UPt_3 to the model scattering cross section $\sigma_n^{\text{cal}} = (\gamma r_0/2)^2\mu^2|\mathbf{q} \times \mathbf{m}_{\mathbf{q}}|^2|f(\mathbf{q})|^2|\mathcal{F}(\mathbf{q})|^2$, where $(\gamma \mathbf{r}_0/2)^2 = 72.65 \times 10^{-3}$ b/μ_B, $\mu = 0.018(2)\mu_B$/U atom, f is the magnetic form factor for uranium, and $\mathcal{F}$ is the normalized structure factor for a magnetic unit cell containing 4 U atoms [25]. Units for σ_n are 10^{-5} b. The resulting reliability coefficient $R = \sum|\sigma_n^{\text{obs}} - \sigma_n^{\text{cal}}|/\sum\sigma_n^{\text{obs}}$ is 29%.

$\mathbf{q}$	σ_n^{obs}	σ_n^{cal}	$\mathbf{q}$	σ_n^{obs}	σ_n^{cal}
(2, −1.5, 0)	16(1)	18.1	(0.5,0,1)	9(1)	6.70
(1.5, −1, 0)	9.9(6)	10.1	(1.5,0,1)	5(2)	8.23
(1,0.5,0)	9.0(8)	10.1	(0.5,0,2)	31(3)	16.2

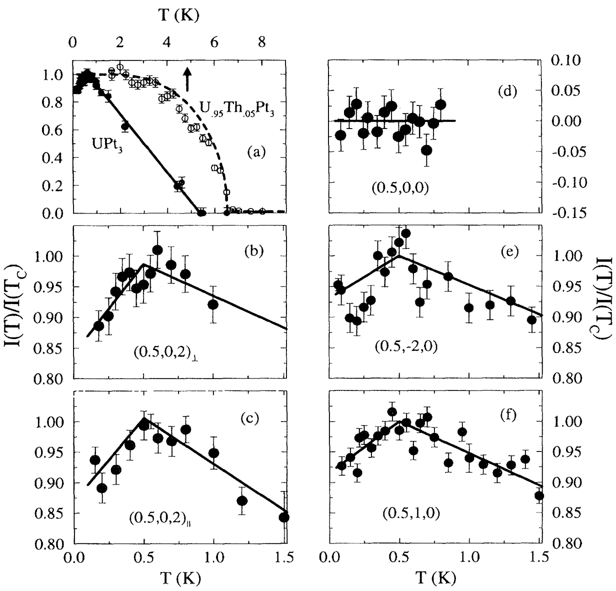

FIG. 3. (a) Antiferromagnetic order parameters for UPt_3 (filled circles) measured with x rays and $U_{0.95}Th_{0.05}Pt_3$ (open circles) measured with neutrons. The dashed line is a mean-field model fit with $S = 1/2$. (b),(c) Integrated intensity of the x-ray magnetic scattering at $\mathbf{q} = (0.5, 0, 2)$ with the $[h, 0, l]$ plane either perpendicular (b) or parallel (c) to the horizontal scattering plane. (d)–(f) Neutron magnetic scattering at $\mathbf{q} = (0.5, 0, 0)$, (0.5,–2,0), and (0.5,1,0). The peak intensity at (0.5,0,0) was normalized to the (0.5,1,0) intensity. The solid lines are linear least-squares fits to the data with $T_c = 0.5$ K.

Néel temperature and the subsequent temperature dependence of the Bragg intensity are similar to what is found in the bulk neutron experiments [11], but very different from the impurity-induced but seemingly conventional appearing antiferromagnetism in $U_{0.95}Th_{0.05}Pt_3$. We conclude that unlike all other central peak phenomena studied with a combination of x-ray and neutron scattering to date [22], with the possible exception of URu_2Si_2 [18,23], the short-range antiferromagnetic order in UPt_3 is unique in that the temperature variation of the order parameter is not substantially dependent on whether we are looking at bulk or near-surface regions.

We now turn to the effects of superconductivity on antiferromagnetic order. Figure 3 shows the temperature dependence of x-ray and neutron diffraction at four different antiferromagnetic Bragg points. Each data set probes the temperature dependence of different projections and Fourier components of the magnetization density: X-ray diffraction measures $\sigma_x \propto |\mathbf{k}_i \cdot \mathbf{m_q}(T)|^2$ ($\mathbf{k}_i$ being the incident wave vector and $\mathbf{q} = \mathbf{k}_f - \mathbf{k}_i$), whereas neutron diffraction measures $\boldsymbol{\sigma}_n \propto |\mathbf{q} \times \mathbf{m_q}(T) \times \mathbf{q}|^2$. Even so, all finite cross sections show a similar temperature dependence displaying a maximum close to T_c followed by a decrease as the superconducting order parameter develops. The magnitude of the decrease for the two orientations of the x-ray measurement and the two reflections of the neutron measurement are the same within the errors. Moreover, magnetic neutron diffraction for $\mathbf{q} = (0.5, 0, 0)$, which in the model corresponding to Fig. 2(d) is absent because $\mathbf{m}_{\mathbf{a}^*/2} \parallel \mathbf{a}^*$, remains absent for $T < T_c$.

These observations suggest that $\mathbf{m_q}(T) \equiv \mu(T)\hat{\mathbf{m}}'_{\mathbf{q}}$, i.e., that the temperature dependence for $T < T_c$ arises solely from the temperature-dependent staggered magnetization, $\mu(T)$. This scenario (Ampl) and two collinear modifications of the antiferromagnetic structure are compared to the relative reductions of the scattering cross sections, $\delta \equiv [\sigma(T_c) - \sigma(0)]/\sigma(T_c)$ in Table II. $\epsilon = 5°$ denotes an unlikely model in which a 5° rotation around $\mathbf{c}^*$ with *definite* handedness occurs below T_c. $|\epsilon| = 5°$ denotes a model in which each orthorhombic domain separates into two equal-sized domains in which moments rotate 5° around $\mathbf{c}^*$ with left and right handedness. It is apparent that both the x-ray and neutron diffraction data rule out a simple rotation of the collinear structure in Fig. 2(d). Instead, the data are consistent with a uniform reduction of the squared staggered magnetization of 11% ± 2% when averaged over all geometries and reflections. The 9% ± 3% reduction of the (0.5,1,0) intensity measured by neutrons for the annealed sample is indistinguishable from the 6.3% ± 0.9% reduction previously measured for an unannealed sample [11]. If we allow for a combined amplitude relation and rotation, we find that the limit on the rotation of the collinear antiferromagnetic structure set by our data is $|\epsilon| < 2°$.

This result can be best understood in the language of a phenomenological Ginzburg-Landau free energy functional in which there is a coupling term of the form [24] $F_{sc\text{-}M} = d_1|\boldsymbol{\eta}|^2|\mathbf{m_q}|^2 + d_2|\boldsymbol{\eta} \cdot \mathbf{m_q}|^2$, and a purely mag-

TABLE II. Relative reduction in the x-ray and neutron magnetic diffraction cross sections at selected Bragg points upon cooling the sample from $T \approx T_c$ to $T = 0$ (see Fig. 3).

	$\Delta\sigma_{\text{x-ray}}/\sigma_{\text{x-ray}}$		$\Delta\sigma_n/\sigma_n$		
$\mathbf{q}$	$(0.5, 0, 2)_\parallel$	$(0.5, 0, 2)_\perp$	$(0.5, 1, 0)$	$(0.5, -2, 0)$	$(0.5, 0, 0)^a$
Observed	0.14(3)	0.15(5)	0.09(3)	0.07(3)	0.00(3)
Ampl	0.11	0.11	0.11	0.11	0
$\epsilon = 5°$	0.01	0.61	0.20	−0.04	−0.04
$\lvert\epsilon\rvert = 5°$	0.01	−0.13	0.00	0.01	−0.04

[a]Normalized to the peak intensity of the (0.5,1,0), magnetic Bragg peak.

netic term $F_M = a|\mathbf{m_q}|^2 + b|\mathbf{m_q}|^4 - D|\mathbf{m_q} \cdot \hat{\mathbf{a}}^*|^2$. The superconducting order parameter $\boldsymbol{\eta}$ is a complex vector in most theories of unconventional superconductivity in UPt_3 [9,10]. The first term in $F_{sc\text{-}M}$ is present for conventional s-wave superconductors, while the second term is unique to unconventional states. The first two terms in F_M represent the free energy of an antiferromagnet, while the last term represents the basal plane anisotropy within an orthorhombic domain. Our result shows that the coupling in $F_{sc\text{-}M}$ is strong enough to suppress, but not rotate, $\mathbf{m_q}$. This in turn indicates that for $H = 0$ either (i) d_1 is much larger than d_2 or (ii) D is much larger than d_2; i.e., the magnetic anisotropy is so large that the superconducting state has no observable effect on the moment orientation. Either case has serious consequences for theories of the split superconducting transition. Scenario (i) taken together with the fact that the temperature dependence of the magnetic order parameter and the magnetic correlation length, $\xi_{\rm AFM}$, are uncorrelated with the presence of the split superconducting transition, and that $\xi_{\rm AFM} \ll \xi_{sc}(T \approx T_c)$, suggests that antiferromagnetism merely plays the conventional pair-breaking role that it plays in s-wave superconductors. In other words, our data raise the question as to whether the weak antiferromagnetic order is in fact the symmetry-breaking field required by most theories to split T_c [9,10,24]. On the other hand, scenario (ii) would allow antiferromagnetism to fulfill the role of symmetry-breaking field, implying a multidomain superconducting state with domain sizes of the order $\xi_{\rm AFM}$ with the superconducting order parameter $\boldsymbol{\eta}$ displaying the anisotropy of each antiferromagnetic domain. Such a random superconducting domain state could yield the broad transition of as-grown samples (see Fig. 1), but it is hard to reconcile with the resolved transitions in the annealed crystals which still have $\xi_{\rm AFM} \ll \xi_{sc}(T \approx T_c)$.

In conclusion, we have used x-ray resonant magnetic and neutron magnetic scattering to show that the superconducting order parameter brings about a reduction in the squared, staggered magnetization without changing the symmetry of the antiferromagnetic order parameter in UPt_3. Of course, we cannot exclude changes of symmetry that would be revealed by new Bragg peaks far from those associated with the basal plane unit cell doubling. The characteristics of the antiferromagnetic order and the influence of superconductivity on the order appear not to depend on whether the specific heat displays a split superconducting transition. Qualitatively, they are also not substantially different for bulk and near-surface regions. It is difficult to reconcile our results with existing theories which attribute the split superconducting transition of UPt_3 to weak antiferromagnetic order. Thus, it is worthwhile to explore other possible symmetry-breaking fields [1] of both structural [19] and magnetic (e.g., quadrupolar) origin for the superconducting order in UPt_3.

We thank P. Gammel, S. Hayden, D. Hess, R. Kleiman, A. Millis, M. Nelson, C. Varma, and H. Williams for helpful discussions, and K. Clausen and J. Kjems for their hospitality at Risø. C. B. is supported by the National Science Foundation through DMR-9453362. ORNL beam line X14A is supported by U. S. DOE Contract No. DE-AC05-840R21400.

*Present address: ETH, 8093 Zurich, Switzerland.
†Also at University of Konstanz, Konstanz, Federal Republic of Germany.

[1] Z. Fisk and G. Aeppli, Science **260**, 38 (1993).
[2] D.J. Bishop *et al.,* Phys. Rev. Lett. **53**, 1009 (1984); B.S. Shivaram *et al.,* Phys. Rev. Lett. **56**, 1078 (1986).
[3] C.L. Broholm *et al.,* Phys. Rev. Lett. **65**, 2062 (1990).
[4] R.N. Kleiman *et al.,* Phys. Rev. Lett. **69**, 3120 (1992).
[5] G. Goll *et al.,* Phys. Rev. Lett. **70**, 2008 (1993).
[6] B. Lussier *et al.,* Phys. Rev. Lett. **74**, 3294 (1994).
[7] R.A. Fisher *et al.,* Phys. Rev. Lett. **62**, 1311 (1989).
[8] A.P. Ramirez, N. Stücheli, and E. Bucher, Phys. Rev. Lett. **74**, 1218 (1995); V. Müller *et al.,* Phys. Rev. Lett. **58**, 1224 (1987); R.N. Kleiman, Phys. Rev. Lett. **62**, 3120 (1992); A. Schenstrom *et al.,* Phys. Rev. Lett. **62**, 332 (1989); .
[9] T. Fujita *et al.,* J. Phys. Soc. Jpn. **1**, 247 (1994), and references therein.
[10] R. Joynt, Supercond. Sci. Technol. **1**, 210 (1988); D.W. Hess *et al.,* J. Phys. Condens. Matter **1**, 8135 (1989); E. Blount, Phys. Rev. Lett. **64**, 3074 (1990); M. Sigrist and K. Ueda, Rev. Mod. Phys. **63**, 239 (1991).
[11] R.H. Heffner *et al.,* Phys. Rev. B **39**, 11 345 (1989); G. Aeppli *et al.,* Phys. Rev. Lett. **60**, 615 (1988).
[12] G. Aeppli *et al.,* Phys. Rev. Lett. **63**, 676 (1989).
[13] S.M. Hayden *et al.,* Phys. Rev. B **46**, 8675 (1992).
[14] G. Luke *et al.,* Phys. Rev. Lett. **71**, 1466 (1993).
[15] T.J. Head *et al.,* Acta Crystallogr. **8**, 494 (1955).
[16] A. Habenshuss *et al.,* Nucl. Instrum. Methods, Phys. Res., Sect. A **266**, 215 (1988).
[17] D. Gibbs *et al.,* Phys. Rev. Lett. **61**, 1241 (1988); E.D. Isaacs *et al.,* Phys. Rev. Lett. **62**, 1671 (1989).
[18] E.D. Isaacs *et al.,* Phys. Rev. Lett. **65**, 3185 (1990); J. Appl. Phys. **76**, 6133 (1994).
[19] P.A. Midgely *et al.,* Phys. Rev. Lett. **70**, 678 (1993).
[20] A.P. Ramirez *et al.,* Phys. Rev. Lett. **57**, 1072 (1986); A. de Visser *et al.,* Phys. Rev. B **34**, 8168 (1986).
[21] A.L. Goldman *et al.,* Phys. Rev. B **34**, 6564 (1986); P.H. Frings *et al.,* J. Magn. Magn. Mater. **63–64**, 202 (1987).
[22] T.R. Thurston *et al.,* Phys. Rev. B **49**, 15 730 (1994), and references therein.
[23] T.E. Mason *et al.,* Phys. Rev. Lett. **65**, 3189 (1990).
[24] R. Joynt, Phys. Rev. Lett. **70**, 678 (1993).
[25] Data in the $(hk0)$ zone were normalized to six weak nuclear Bragg peaks not subject to extinction. The absolute cross sections for magnetic Bragg peaks in the $(h0l)$ zone may be overestimated by as much as 30% because a long axis of the crystal was in the scattering plane and the (100) nuclear Bragg peak used for normalization in that zone may have been subject to secondary extinction.